Research Article Vol. 31, No. 5 / 27 Feb 2023 / Optics Express 8998
Optics EXPRESS

Intracavity-loss controlled wavelength-tunable bidirectional mode-locked erbium-doped fiber laser

LILONG DAI,[1] ZINAN HUANG,[1] QIANQIAN HUANG,[1] MOHAMMED AL ARAIMI,[2] ALEKSEY ROZHIN,[3] XINDONG LIANG,[4,5] AND CHENGBO MOU[1,*]

[1]*The Key Lab of Specialty Fiber Optics and Optical Access Network, Shanghai Institute for Advanced Communication and Data Science, Joint International Research Laboratory of Specialty Fiber Optics and Advanced Communication, Shanghai University, Shanghai, 200444, China*
[2]*Department of Engineering, University of Technology and Applied Sciences (Higher College of Technology), PO Box 74, Al-Khuwair, Postal Code 133, Sultanate of Oman*
[3]*Aston Institute of Photonic Technologies (AIPT), Aston University, Birmingham B4 7ET, UK*
[4]*Key Laboratory of Gravitational Wave Precision Measurement of Zhejiang Province, Hangzhou Institute for Advanced Study, UCAS, Hangzhou 310024, China*
[5]*Zhejiang Lab, Hangzhou, 311100, China*
[*]*mouc1@shu.edu.cn*

Abstract: Bidirectional wavelength-tunable mode-locked fiber lasers have demands for many applications. In our experiment, two frequency combs from a single bidirectional carbon nanotube mode-locked erbium-doped fiber laser are obtained. Continuous wavelength tuning is demonstrated in the bidirectional ultrafast erbium-doped fiber laser for the first time. We utilized the microfiber assisted differential loss-control effect on both directions to tune operation wavelength and it presents different wavelength tuning performances in two directions. Correspondingly, the repetition rate difference can be tuned from 98.6 Hz to 32 Hz by applying strain on microfiber within 23 μm stretching length. In addition, a minor repetition rate difference variation of 4.5 Hz is achieved. Such technique may provide possibility to expand wavelength range of dual-comb spectroscopy and broad its application fields.

1. Introduction

Bidirectional mode-locked fiber lasers perform as special optical sources that two ultrashort pulses can be generated simultaneously in both clockwise (CW) and counter clockwise (CCW) direction. Their compact system and outstanding output characteristics have acquired massive attention and found applications in optical sensing, dual-comb spectroscopy, terahertz spectroscopy, *etc* [1–6]. Besides, bidirectional mode-locked fiber lasers also offer new platform for mode locking dynamics study [7,8]. Therefore, many efforts have been devoted to realize bidirectional mode-locked fiber laser operating at different wavelength range under various operation regime [9–13]. Among them, the most attractive property is the mutual coherence and common noise cancellation in bidirectional mode-locked fiber laser, from which two coherent frequency combs with a slight repetition rate difference (Δf_{rep}) can be produced for dual-comb spectroscopy application.

One type of bidirectional dual-comb fiber lasers tends to focus on two-branch structure. But the small Δf_{rep} depends on two cavity length difference, which is hard to accomplish and adjust. On the other hand, counter-propagating pulses emitted from a single ring cavity is more promising due to simple constructure and cost effectiveness. In Ref. [14] and [15], Mehravar *et al* and Olson *et al* separately successfully exploited a bidirectional mode-locked erbium-doped and thulium-doped fiber laser to apply them for absorption measurement. However, these dual-comb systems always operate at a fixed wavelength. Increasing operation wavelength can expand

#481788 https://doi.org/10.1364/OE.481788
Journal © 2023 Received 24 Nov 2022; revised 7 Jan 2023; accepted 22 Jan 2023; published 24 Feb 2023

Optics EXPRESS

absorption measurement range in dual comb spectroscopy. Zeng *et al* and Yao *et al* utilized the intrinsic fiber birefringence effect in bidirectional mode-locked fiber laser, in which central wavelength of the counter-propagating pulses can be modified by changing cavity length and fiber birefringence [16,17]. But such polarization controllers adjustment method will result in a discrete and rough control of wavelength [18]. So far, precise and continuous wavelength tuning or controlling in bidirectional mode-locked fiber laser is challenging and has rarely been demonstrated. In other words, a suitable wavelength tuning mechanism is in demand.

Microfibers are of great interest for a range of emerging fiber optic applications, including optical sensing, nonlinear optics, optical trapping, *etc*. for their outstanding properties of large evanescent field, high nonlinearity, strong confinement and low loss interconnection [19]. More importantly, microfiber-based fiber device also finds extensive applications in fiber lasers. For instance, Luo *et al* demonstrated a femtosecond mode-locked fiber laser by using the evanescent field interaction between microfiber and few-layer black phosphorus [20], Liu *et al* proposed a graphene decorated microfiber knot resonator to achieve four wave mixing effect for ultrahigh repetition rate pulse generation [21]. In addition, microfiber can also perform as an effective continuous wavelength tuning element in fiber laser, for their merits of fine controlling, all fiber configuration, low loss insertion, ease of fabrication, *etc*. Fang *et al* reported a wavelength-tunable mode-locked fiber laser operating at 2 μm, in which a microfiber filter with intermodal interference induced quasi-sinusoidal transmission spectra is applied as a wavelength selection element [22]. The large extinction ratio (ER) guarantees perfect spectral shaping and fine wavelength selectivity in the unidirectional mode-locked fiber laser. However, it is worth to notice that these strong wavelength selection function of the filter will result in the phenomena that the counter-circulating pulses will possess the same operation wavelength and tuning tendency in a single bidirectional mode-locked fiber laser [23,24], which is not suitable for dual-comb spectroscopy. Hence, an alternative wavelength tuning mechanism is necessary to realize continuously spectral tuning from single bidirectional mode-locked fiber laser, in which two pulses own different repetition frequency. Another type of continuous wavelength tuning mechanism is based on the loss control capability. Feng *et al* exploited a microfiber based variable attenuator and realized continuous wavelength tuning with reverse strain [25]. Nevertheless, large loss change during bending will weak mode locking performance and even break mode locking states, especially in bidirectional fiber laser that gain competition exists. In essence, the microfiber assisted filter effect can also be attributed to loss adjustment imposed on gain profile. The emission wavelength in fiber laser is also decided by the combination effect between loss and gain. Consequently, a microfiber with a small ER in transmission would be inherently capable of breaking strong wavelength selection function but controlling emission wavelength in a small loss adjusting manner between the two opposite directions.

In this work, a bidirectional wavelength-tunable mode-locked erbium-doped fiber laser was reported. Two frequency combs with a slight Δf_{rep} from a single cavity is demonstrated. The same cavity perturbations between two pulses ensure small variation of 4.5 Hz in Δf_{rep} and further pave the road to dual-comb spectroscopy applications. Besides, by stretching the microfiber, it induces differential loss controlling effect for the counter-propagating pulses, and wavelength tuning is achieved in both CW and CCW directions with distinct performance. Such phenomena result in a tunable Δf_{rep} from 98.6 Hz to 32 Hz and it can be decreased below the anti-aliasing value of 38.9 Hz. This helps direct dual-comb spectroscopy application within the whole spectra without extra spectral filter. Moreover, the wavelength tuning performance also may expand operation wavelength range and broad dual comb spectroscopy applications fields.

2. Experimental setup

The experimental diagram of bidirectional wavelength-tunable mode-locked fiber laser is shown in Fig. 1(a). We choose the HiPco single walled carbon nanotube (SWCNT) and uniformly disperse

Optics EXPRESS

it in the polyvinyl alcohol (PVA) matrix. The SWCNT diameter distribution of 0.8-1.2 nm guarantees the considerable optical absorption in the communication band, and the highly optical transmissive polymer matrix also facilitates the role of SWCNT-PVA polymer composite as an intensity discriminator in the erbium-doped fiber laser. The detailed fabrication procedure and characteristics can be found in Ref. [26]. A section of erbium-doped fiber (OFS EDF80) with a length of 114 cm provides gain to the laser, which has a group velocity dispersion (GVD) of +63.8 ps^2/km. The laser emission is pumped by a 976 nm laser source through a 980/1550 nm wavelength division and multiplexer composed of HI1060 fiber pigtails. The HI1060 fiber owns length of ~ 200 cm and GVD of -7 ps^2/km. For intracavity pulse stabilization, an in-line mechanical polarization controller (PC) is applied. We extract 20% optical signals outside the cavity for further analysis via an 2×2 optical coupler (OC). To avoid any unwanted reflected optical signals, we utilize two polarization insensitive isolators in each direction outside the cavity. Wavelength tuning is achieved by insertion of a microfiber which is fixed on a high-resolution three-dimension displacement platform (Thorlab Nanomax300). The microfiber is fabricated with single mode fiber (Coring SMF28e) by standard flame brush technique, and the conical structure can be formed during heating and stretching process [27]. Higher order cladding mode can be excited when diameter is decreased resulting in modal interference. Figure 1(b) displays the transmission spectra of the fabricated microfiber with a free spectral range (FSR) of 15 nm and ER of 0.43 dB. The quasi-sinusoidal response indicates that primarily two modes are excited. The transmission spectrum will blue shift as a result of increased intermodal interference interaction

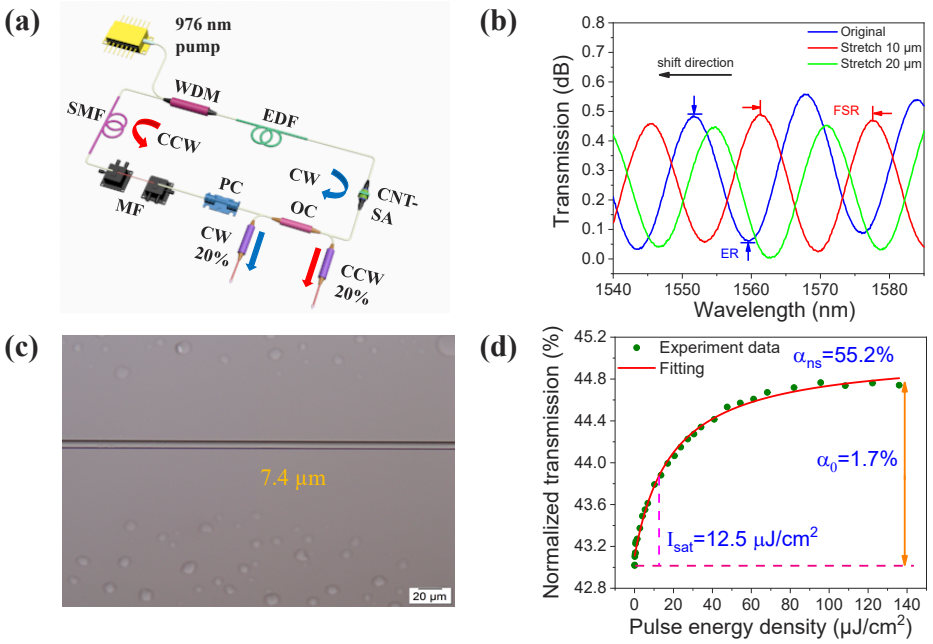

Fig. 1. Experiment setup and device characteristics. (a) experimental diagram of the bidirectional wavelength-tunable mode-locked erbium-doped fiber laser, WDM: wavelength division and multiplexer, EDF: erbium-doped fiber, CNT-SA: carbon nanotube saturable absorber, OC: optical coupler, PC: polarization controller, MF: microfiber, SMF: single mode fiber, CW: clockwise, CCW: counter-clockwise. (b) transmission spectrum of microfiber, ER: extinction ratio, FSR: free spectral range. (c) microscopy image of microfiber. (d) nonlinear optical absorption of CNT-SA, α_0: modulation depth, α_{ns}: non-saturable loss, I_{sat}: saturable pulse energy.

Optics EXPRESS

length. The microscopy image of microfiber is shown in Fig. 1(c) and the diameter is 7.4 μm with high uniformity. Here we exploit such microfiber with a relatively small ER, for the reason that a larger value will result in a strong spectral filter effect. And such effect will eliminate the repetition frequency difference of two frequency combs, as well as lead to synchronization between two ultrafast pulses which is not suitable for dual-comb spectroscopy. The pigtails of other optical components and the remaining of cavity are both SMF. The total cavity length is estimated to be ~13 m and the calculated net dispersion is about -0.168 ps^2 corresponding to the conventional soliton operation regime. The nonlinear optical absorption characteristics of CNT-SA was measured and displayed in Fig. 1(d). The modulation depth α_0 reaches 1.7% indicating effective SA function. Besides, non-saturable loss and saturable energy of CNT-SA are 55.2% and 12.5 μJ/cm^2, respectively.

3. Results & discussion

Mode locking is easy to achieve both in the CW and CCW direction and we find the threshold to produce pulse in the CW direction is slightly smaller than that in the CCW direction. This is attributed to the asymmetric design of the cavity that pump light is directly absorbed by the gain medium in the CW direction, while the light is attenuated by the OC and CNT-SA from the opposite direction. Coarse adjustment of PC and pump power are applied to achieve stable single pulse operation from both directions. When pump power was set at 30 mW, Fig. 2(a) displays the typical output spectra of counter-circulating pulses by an optical spectrum analyzer (OSA) (Yokogawa AQ6370D) and it is clear to see that the central wavelength from CW and CCW direction is 1566.36 nm and 1569.78 nm, respectively. The asymmetric configuration and gain competition effect are responsible for the operation wavelength difference. Besides, the full width of half maximum (FWHM) reaches 6.32 nm in the CW direction and 5.88 nm in the CCW direction. The obvious Kelly sidebands in the optical spectrum is obtained by soliton mode locking. To further analyze the output characteristics of the laser, optical pulses are transferred to the electrical signals with a 12.5 GHz bandwidth photodetector (Newport 818-BB-51F), and directly observed from a 4 GHz bandwidth high-speed real-time oscilloscope (Keysight DSOS404A) and an electrical spectrum analyzer (Rohde & Schwarz FSV-30). Figure 2(b) shows the pulse trains in the CCW direction with a time interval of 65.44 ns. The equally spaced single electrical line and minor intensity disturbance indicates stable pulse formation. Moreover, the electrical signals in the radio frequency (RF) domain are also presented in Fig. 2(c) with a frequency span of 3.7 MHz and a RBW of 20 Hz.

The fundamental repetition rate of pulse from CCW direction is ~15.282 MHz, which is well fitted with the reciprocal of the pulse spacing in Fig . 2(b). This is also verified by the cavity length that single pulse is produced in the CCW direction. In addition, the signal to noise ratio (SNR) reaches 85 dB and the inset of Fig. 2(c) displays a relatively gentle and minute intensity decrease from the fundamental repetition rate to its high order harmonics over 1 GHz span. These performances are also observed in the CW direction and demonstrate both stable single pulse generation. Figure 2(d) depicts the autocorrelation traces of pulses from two directions with the utilization of a background-free SHG-type autocorrelator (Femtochrome Research FR-103XL). The inset displays experimental data in the CW and CCW direction and they are both well nonlinear fitted by a $Sech^2$ function. The measured pulse duration is 836 fs in the CW direction and 708 fs in the CCW direction.

The two frequency combs generated from a single cavity will possess a slight Δf_{rep} due to their distinct operation wavelength. To monitor these characteristics, we combined two pulses from two directions via a 50:50 OC. Figure 3(a) shows RF spectrum of combined signals over a frequency span of 5 kHz and RBW of 1 Hz. It is clear that the fundamental repetition rate locates at 15.2826075 MHz in the CW direction and 15.2825235 MHz in the CCW direction. The newly generated RF combs characterize a line spacing Δf_{rep} of 84 Hz. The corresponding

Optics EXPRESS

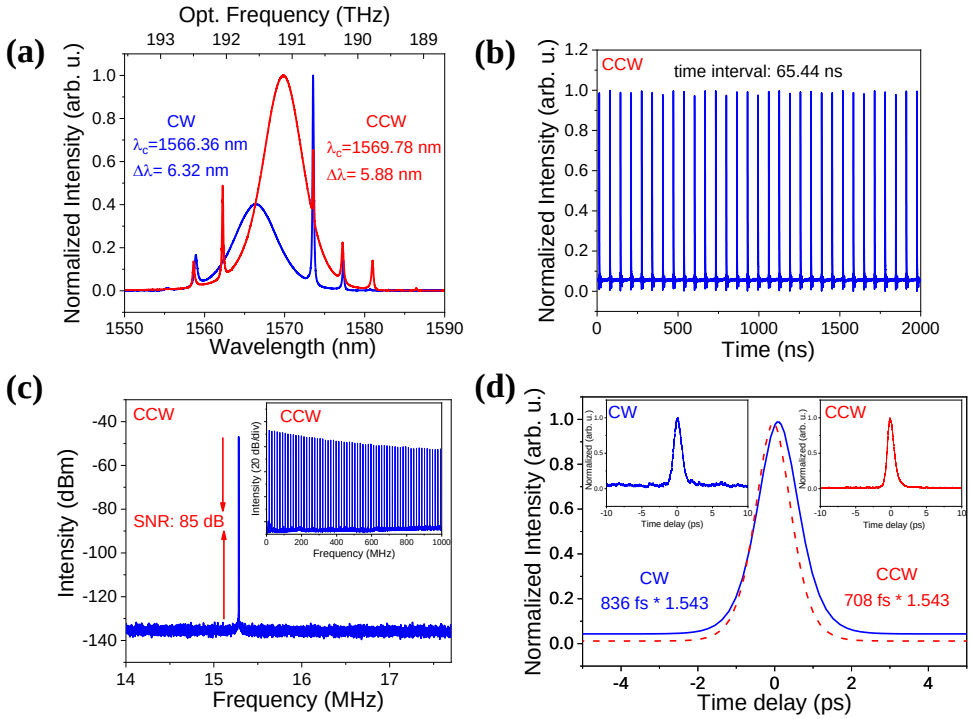

Fig. 2. The output characteristics of pulses from two directions. (a) optical spectra of the counter-circulating pulses; (b) pulse trains from CCW direction in the time domain; (c) radio frequency spectrum in the CCW direction, inset: the fundamental repetition rates and its high order harmonics in the CCW direction over 1 GHz span; (d) the autocorrelation curves fitted by hyperbolic secant function in the CW and CCW directions, inset: measured experimental data of autocorrelation curves in the CW and CCW directions.

periodic interferograms in the time domain is also demonstrated in Fig. 3(b), and the measured period of beat note waveform is 11.74 ms, which also corresponding to the Δf_{rep}. Besides, we also monitor the frequency stability per one minute during 40 minutes as displayed in Fig. 3(c). The fundamental frequency of counter-propagating pulses performs relatively large change over time and mainly caused by the environmental disturbance. However, since two lasers share the same cavity and suffer same perturbation, the variations in repetition frequency are cancelled and can lead to the relatively stable Δf_{rep}. The small variation of 4.5 Hz also confirms the possibility in dual-comb spectroscopy applications. We demonstrated preliminary dual-comb spectroscopy with this fiber laser and the results are enclosed in Supplement 1.

In our experiment, we find that the operation wavelength can be tuned by stretching the microfiber. We notice that the emission wavelength from the opposite direction show different response to the microfiber stretching. Here we set the home position of microfiber when the output wavelength in the CCW direction reaches its maximum. Fig . 4(a) exhibits wavelength tuning performance and the corresponding fundamental repetition rates of the counter-circulating pluses. The central wavelength versus displacements in the CCW direction is from 1570.46 nm to 1567.18 nm within 23 μm displacements range and appears approximately linear manner. While in the CW direction, it presents an enveloping change curve where the wavelength increases from 1566.36 nm to 1567.58 nm and decreases to 1566.08 nm. Such wavelength variations also contribute to the relative repetition frequency change between two directions, and their

Optics EXPRESS

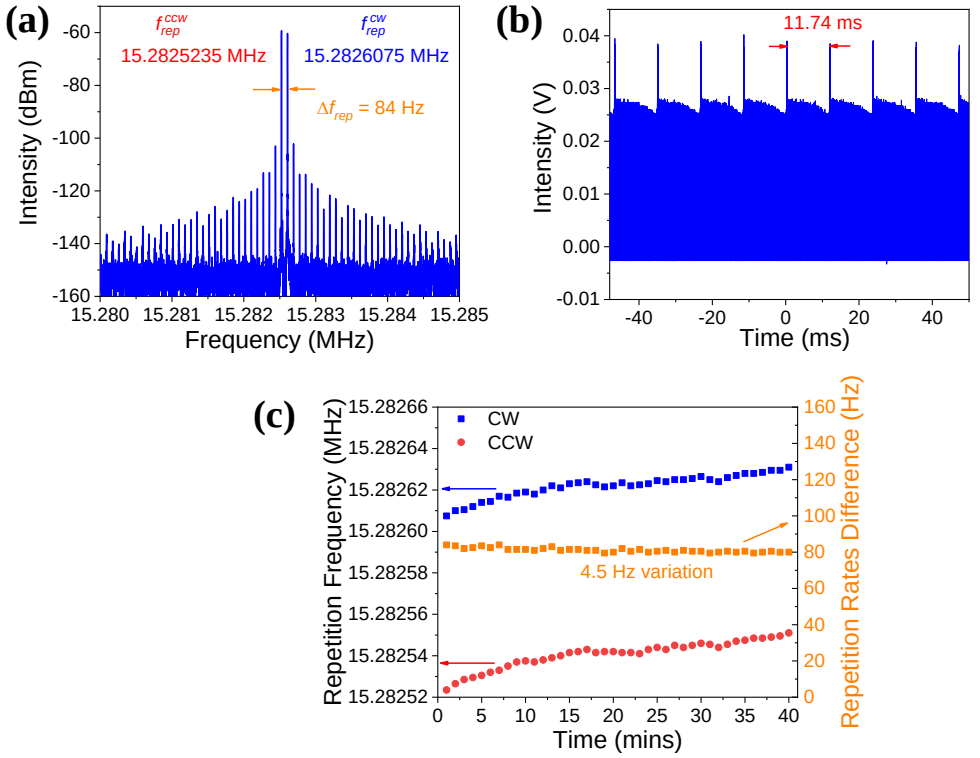

Fig. 3. The combined output pulses characteristics. (a) signals in the radio frequency domain; (b) signals in the time domain; (c) stability of fundamental frequency and repetition rates difference Δf_{rep}.

relationships are also shown in Fig. 4(a). Due to the small ER of 0.43 dB of microfiber, we believe that the wavelength tuning mechanism should be attributed to the differential loss induced by the sinusoidal spectrum rather than spectral filtering. This is also confirmed that the counter-propagating pulses possess different operation wavelength. To figure out the specific mechanism of wavelength tuning, we measured the transmission spectrum of microfiber at home position (zero displacement) as shown in Fig. 4(b), where the laser wavelength locates at the falling edge of transmission window of the microfiber for the CW direction, and trough for the CCW direction. While applying continuous strain on microfiber in the laser, we measured a set of transmission spectra under every displacement. The corresponding insertion loss of the microfiber at each operation wavelength versus every displacement is also monitored, which are described in Fig. 4(c) and (d). The results illustrate that the increased insertion loss will result in a blue wavelength shift for the reason that shorter wavelength will experience larger gain [28]. Hence, the loss control function of microfiber is verified and responsible for such wavelength tuning performances. Besides, we find that the insertion loss change curve of microfiber versus displacements from two directions can be fitted with the transmission curve in the blue and red spectral window, respectively. The loss induced wavelength tuning performance will be depended on and follow the transmission profile from left to right, because the transmission spectrum will blue shift upon stretching as shown in Fig. 1(b). This feature may help us to further realize diverse wavelength tuning tendency by adjusting original location in the transmission curve of the counter-propagating pulses. This can be optimized with further microfiber design, cavity polarization and pump modification.

Optics EXPRESS

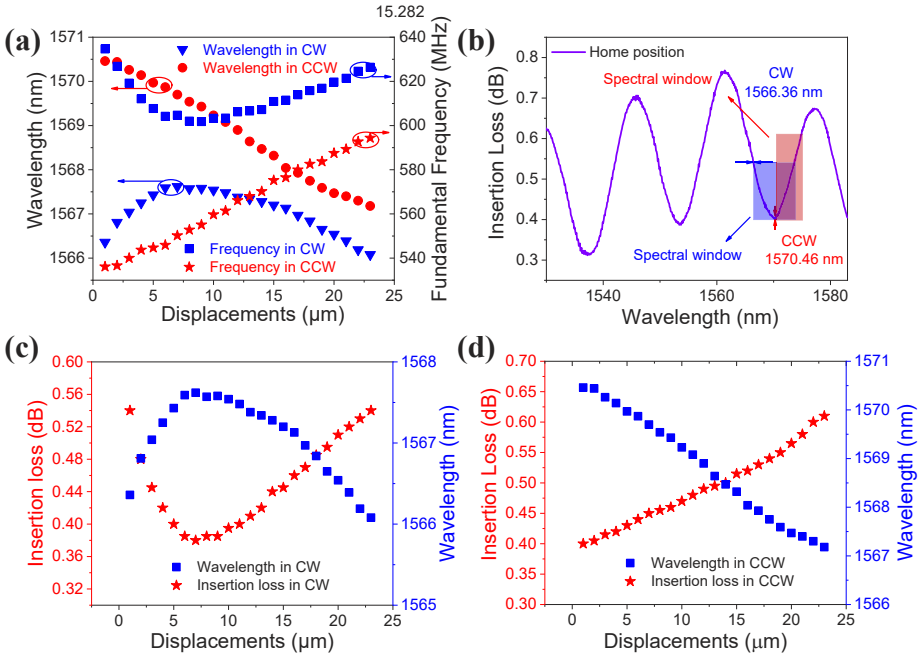

Fig. 4. wavelength tuning characteristics versus microfiber displacements. (a) wavelength and fundamental repetition rate change versus displacements in the opposite directions. (b) the home position of microfiber that wavelength tuning is obtained. (c) insertion loss of microfiber and the corresponding operation wavelength versus displacement in the CW direction. (d) insertion loss of microfiber and the corresponding operation wavelength versus displacement in the CCW direction.

When further stretching the microfiber, mode locking will disappear in the CCW direction and we attribute it to the excessive loss exerted by microfiber. More importantly, their different tuning performance versus displacements holds the possibility to tune Δf_{rep} as shown in Fig. 5(a). And we find that the Δf_{rep} between two frequency combs can be tuned from 98.6 Hz to 32 Hz exponentially. In dual-comb spectroscopy application, to maintain one to one mapping between both modes of optical and RF combs, the condition $\Delta f_{opt} < f_{rep}^2 / 2\Delta f_{rep}$ must to be satisfied [29–31]. When the fundamental repetition rates f_{rep} locates at ~15.282 MHz and the repetition rate difference Δf_{rep} is 84 Hz, the calculated anti-aliasing optical frequency width Δf_{opt} should be 1.39 THz, which does not cover the full optical spectrum as shown in Fig. 2(a). For further dual-comb spectroscopy application, an external spectral filter is required to avoid spectral aliasing. [5]. Considering a maximum optical frequency bandwidth of about 3 THz in our experiment, the calculated anti-aliasing Δf_{rep} should be 38.9 Hz. When the displacement reaches 13 μm and larger, the aliasing effect can be eliminated and the whole spectra can be observed without bandpass filter. Figure 5(b) depicts the fundamental frequency and Δf_{rep} versus pump current. When laser diode currents increase, the repetition frequency in the CW direction will increase but decrease in the CCW direction. Besides, the magnitude of Δf_{rep} increases with increased pump current and the change is almost linear. These tunable properties may be useful for feedback control of Δf_{rep} in the future. The decreased Δf_{rep} below anti-aliasing value can help to broad the bandwidth of dual-comb spectroscopy. In addition, the wavelength tuning may also provide possibility to achieve multi-operation wavelength of dual-comb spectroscopy and expand their applications range.

Optics EXPRESS

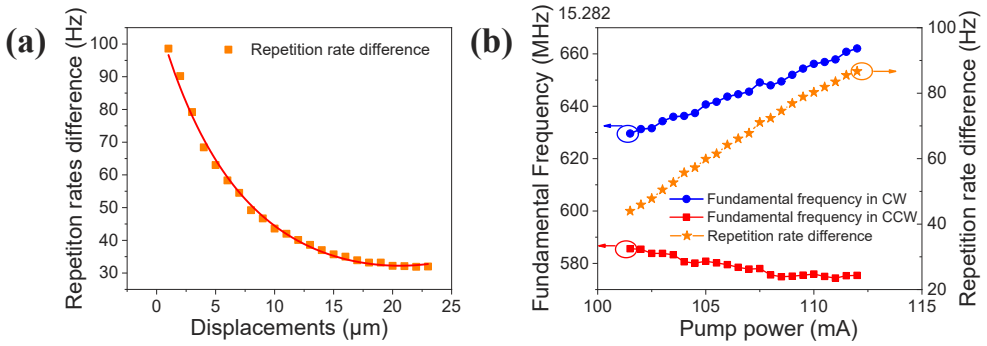

Fig. 5. Repetition rate variation characteristics. (a) repetition rate difference Δf_{rep} versus displacement. (b) fundamental frequency and Δf_{rep} versus pump power.

4. Conclusions

In conclusion, a bidirectional loss-controlled wavelength-tunable mode-locked erbium-doped fiber laser is demonstrated. Two mutually coherent frequency combs are simultaneously generated from a single cavity with small variable Δf_{rep} of 4.5 Hz. Besides, the wavelength from the opposite directions can be both tuned by imposing strain on microfiber. The periodic loss curve of microfiber will induce differential loss effect in the counter-propagating pulses, and then result in distinct wavelength tuning range and trend. In the CW direction, operation wavelength is firstly increased from 1566.36 nm to 1567.58 nm and further decreased to 1566.08 nm, while in the CCW direction, the wavelength tuning is achieved from 1570.46 nm to 1567.18 nm with an approximately linear manner. Such features lead to a tunable Δf_{rep} from 98.6 Hz to 32 Hz, which can be decreased below the anti-aliasing value and help dual-comb spectroscopy applications within a whole optical spectrum. Moreover, the tunable wavelength also provides possibility to obtain multi operation states in dual-comb spectroscopy and enlarge its applications ranges.

Funding. National Natural Science Foundation of China (61975107); Zhejiang Lab Open Research fund (K2022MH 0AB01); Center-initiated Research Project of Zhejiang Lab (K2022MH0AL05).

Acknowledgement. The authors would like to thank Dr. Haochen Tian from The University of Electro-Communications and Prof. Chenglin Gu from East China Normal University for very helpful discussion.

Disclosures. The authors declare no conflicts of interest.

Data availability. Data underlying the results presented in this paper are not publicly available at this time but may be obtained from the authors upon reasonable request.

Supplemental document. See Supplement 1 for supporting content.

References

1. W. Zhang, L. Zhan, T. Xian, and L. Gao, "Bidirectional dark-soliton fiber lasers for high-sensitivity gyroscopic application," Opt. Lett. **44**(16), 4008–4011 (2019).
2. A. A. Krylov, D. S. Chernykh, and E. D. Obraztsova, "Colliding-pulse hybridly mode-locked erbium-doped all-fiber soliton gyrolaser," Laser Phys. **28**(1), 015103 (2018).
3. S. Saito, M. Yamanaka, Y. Sakakibara, E. Omoda, H. Kataura, and N. Nishizawa, "All-polarization-maintaining Er-doped dual comb fiber laser using single-wall carbon nanotubes," Opt. Express **27**(13), 17868–17875 (2019).
4. R. D. Baker, N. T. Yardimci, Y.-H. Ou, K. Kieu, and M. Jarrahi, "Self-triggered asynchronous optical sampling terahertz spectroscopy using a bidirectional mode-locked fiber laser," Sci. Rep. **8**(1), 14802–8 (2018).
5. M. I. Kayes, N. Abdukerim, A. Rekik, and M. Rochette, "Free-running mode-locked laser based dual-comb spectroscopy," Opt. Lett. **43**(23), 5809–5812 (2018).
6. K. Kieu and M. Mansuripur, "All-fiber bidirectional passively mode-locked ring laser," Opt. Lett. **33**(1), 64–66 (2008).
7. Y. Zhou, Y.-X. Ren, J. Shi, and K. K. Wong, "Breathing Dissipative Soliton Molecule Switching in a Bidirectional Mode-Locked Fiber Laser," Adv. Photonics Res. **3**(4), 2100318 (2022).

Optics EXPRESS

8. Y. Yu, C. Kong, B. Li, J. Kang, Y.-X. Ren, Z.-C. Luo, and K. K. Y. Wong, "Behavioral similarity of dissipative solitons in an ultrafast fiber laser," Opt. Lett. **44**(19), 4813–4816 (2019).
9. V. Mamidala, R. Woodward, Y. Yang, H. Liu, and K. K. Chow, "Graphene-based passively mode-locked bidirectional fiber ring laser," Opt. Express **22**(4), 4539–4546 (2014).
10. M. Chernysheva, M. Al Araimi, H. Kbashi, R. Arif, S. V. Sergeyev, and A. Rozhin, "Isolator-free switchable uni-and bidirectional hybrid mode-locked erbium-doped fiber laser," Opt. Express **24**(14), 15721–15729 (2016).
11. Y. Luo, B. Liu, Y. Xiang, Z. Yan, Y. Qin, Q. Sun, and X. Tang, "L-Band Noise-Like Pulse Generation in a Bidirectional Mode-Locked Fiber Laser," IEEE Photon. Technol. Lett. **30**(14), 1333–1336 (2018).
12. B. Li, J. Xing, D. Kwon, Y. Xie, N. Prakash, J. Kim, and S.-W. Huang, "Bidirectional mode-locked all-normal dispersion fiber laser," Optica **7**(8), 961–964 (2020).
13. C. Ouyang, P. Shum, K. Wu, J. H. Wong, H. Q. Lam, and S. Aditya, "Bidirectional passively mode-locked soliton fiber laser with a four-port circulator," Opt. Lett. **36**(11), 2089–2091 (2011).
14. S. Mehravar, R. A. Norwood, N. Peyghambarian, and K. Kieu, "Real-time dual-comb spectroscopy with a free-running bidirectionally mode-locked fiber laser," Appl. Phys. Lett. **108**(23), 231104 (2016).
15. J. Olson, Y. Ou, A. Azarm, and K. Kieu, "Bi-directional mode-locked thulium fiber laser as a single-cavity dual-comb source," IEEE Photon. Technol. Lett. **30**(20), 1772–1775 (2018).
16. X. Yao, "Generation of bidirectional stretched pulses in a nanotube-mode-locked fiber laser," Appl. Opt. **53**(1), 27–31 (2014).
17. C. Zeng, X. Liu, and L. Yun, "Bidirectional fiber soliton laser mode-locked by single-wall carbon nanotubes," Opt. Express **21**(16), 18937–18942 (2013).
18. N. Abdukerim, M. I. Kayes, A. Rekik, and M. Rochette, "Bidirectional mode-locked thulium-doped fiber laser," Appl. Opt. **57**(25), 7198–7202 (2018).
19. G. Brambilla, F. Xu, P. Horak, Y. Jung, F. Koizumi, N. P. Sessions, E. Koukharenko, X. Feng, G. S. Murugan, J. S. Wilkinson, and D. J. Richardson, "Optical fiber nanowires and microwires: fabrication and applications," Adv. Opt. Photon. **1**(1), 107–161 (2009).
20. Z.-C. Luo, M. Liu, Z.-N. Guo, X.-F. Jiang, A.-P. Luo, C.-J. Zhao, X.-F. Yu, W.-C. Xu, and H. Zhang, "Microfiber-based few-layer black phosphorus saturable absorber for ultra-fast fiber laser," Opt. Express **23**(15), 20030–20039 (2015).
21. M. Liu, R. Tang, A.-P. Luo, W.-C. Xu, and Z.-C. Luo, "Graphene-decorated microfiber knot as a broadband resonator for ultrahigh-repetition-rate pulse fiber lasers," Photon. Res. **6**(10), C1–C7 (2018).
22. Q. Fang, K. Kieu, and N. Peyghambarian, "An All-Fiber 2 μm Wavelength-Tunable Mode-Locked Laser," IEEE Photonics Technol. Lett. **22**(22), 1656–1658 (2010).
23. B. Lu, C. Zou, Q. Huang, Z. Huang, M. AlAraimi, C. Mou, Z. Luo, and A. Rozhin, "Wavelength-tunable bidirectional passively Q-switched Er-doped fiber laser incorporating a single-walled carbon nanotube and tunable bandpass filter," Appl. Opt. **59**(9), 2709–2714 (2020).
24. L. Dai, Z. Huang, Q. Huang, M. Alaraimi, A. Rozhin, Z.-C. Luo, and C. Mou, "Microfiber Controlled Bidirectional Wavelength-tunable Mode-locked Fiber Laser Based on Carbon Nanotubes," in *CLEO-PR* 2020 (IEEE, 2020), pp. C5H-3.
25. Y. Feng, X. Li, S. Zhang, M. Han, J. Liu, and Z. Yang, "Wavelength Tunable Q-Switched Fiber Laser Using Variable Attenuator Based on Tapered Fiber," IEEE Photon. Technol. Lett. **29**(24), 2175–2178 (2017).
26. B. Lu, C. Zou, Q. Huang, Z. Yan, Z. Xing, M. Al Araimi, A. Rozhin, K. Zhou, L. Zhang, and C. Mou, "Widely Wavelength-Tunable Mode-Locked Fiber Laser Based on a 45°-Tilted Fiber Grating and Polarization Maintaining Fiber," J. Lightwave Technol. **37**(14), 3571–3578 (2019).
27. T. A. Birks and Y. W. Li, "The shape of fiber tapers," J. Lightwave Technol. **10**(4), 432–438 (1992).
28. M. Melo, O. Frazao, A. Teixeira, L. Gomes, J. Ferreira da Rocha, and H. Salgado, "Tunable L-band erbium-doped fibre ring laser by means of induced cavity loss using a fibre taper," Appl. Phys. B **77**(1), 139–142 (2003).
29. J. Nürnberg, C. G. Alfieri, Z. Chen, D. Waldburger, N. Picqué, and U. Keller, "An unstabilized femtosecond semiconductor laser for dual-comb spectroscopy of acetylene," Opt. Express **27**(3), 3190–3199 (2019).
30. I. Coddington, W. C. Swann, and N. R. Newbury, "Coherent multiheterodyne spectroscopy using stabilized optical frequency combs," Phys. Rev. Lett. **100**(1), 013902 (2008).
31. S. Okubo, K. Iwakuni, H. Inaba, K. Hosaka, A. Onae, H. Sasada, and F.-L. Hong, "Ultra-broadband dual-comb spectroscopy across 1.0–1.9 μm," Appl. Phys. Express **8**(8), 082402 (2015).